ISSN 1070-3284, Russian Journal of Coordination Chemistry, 2015, Vol. 41, No. 8, pp. 524–531. © Pleiades Publishing, Ltd., 2015.

Two Supramolecules Constructed from 2-*o*-Chlorophenylimidazole Dicarboxylate: Syntheses, Crystal Structures, and Thermal Properties[1]

M. J. Yao, X. Ren, Z. F. Yue, and G. Li*

College of Chemistry and Molecular Engineering, Zhengzhou University, Zhengzhou, 450001 P.R. China

**e-mail: gangli@zzu.edu.cn*

Received December 15, 2014

Abstract—Two mononuclear complexes, $[M(o\text{-}ClPhH_2IDC)_2(H_2O)_2] \cdot 4H_2O$ (o-$ClPhH_2IDC$ = 2-(*o*-chlorophenyl)-1*H*-imidazole-4,5-dicarboxylicacid; M = Co(I) and Mn(II)), have been solvothermally synthesized and structurally characterized by single crystal X-ray diffraction (CIF files CCDC nos. 1036900 (**I**) and 1036899 (**II**)), elemental analyses, IR spectroscopy, and powder X-ray diffractionIn both supramolecules, the $[Co(o\text{-}ClPhH_2IDC)_2(H_2O)_2]$ or $[Mn(o\text{-}ClPhH_2IDC)_2(H_2O)_2]$ units are joined through the π–π interactions and intermolecular hydrogen bonds to form the 3D solid-state architectures. Their thermal properties under are have been investigated as well.

DOI: 10.1134/S1070328415070015

INTRODUCTION

Recently, along with the progresses in the field of coordination chemistry, more and more supramolecules with fascinating architectures and potential application in photoluminescence, magnetism, gas storage, ion exchange and catalysis [1–4]. Consequently, a great number of supramolecules showing one-dimensional (1D) chains [5] and ladders [6], two-dimensional (2D) grids [7], three-dimensional (3D) interpenetrated [8] and helical networks [9] have been investigated.

For the construction of supramolecular complexes, the key is to select a powerful organic ligand [10–12], which is helpful to form weak intra- and intermolecular H bonds, and π–π stacking effects. As well known, 1*H*-imidazole-4,5-dicarboxylic acid (H_3IDC) [13, 14] has been proved as an outstanding ligand not only for the possession of six coordination sites: two imidazole nitrogen atoms and four carboxylate oxygen atoms, but also for its potential ability as hydrogen-bonding donors and acceptors [15–20]. To enhance the π–π stacking effects of H_3IDC, our laboratory has paid much concern on the functionalized imidazole dicarboxylate ligands bearing 2-position aromatic groups and designed a series of efficient related ligands successfully.

Hence, 2-(2-chlorophenyl)-1*H*-imidazole-4,5-dicarboxylic acid (o-$ClPhH_3IDC$) is designed and prepared. In this study, we will investigate the reactions of the o-$ClPhH_3IDC$ ligand with transition metals, namely Co(II) and Mn(II) under solvothermal conditions. Fortunately, two supramolecular complexes, $[Co(o\text{-}ClPhH_2IDC)_2(H_2O)_2] \cdot 4H_2O$ (**I**) and $[Mn(o\text{-}ClPhH_2IDC)_2(H_2O)_2] \cdot 4H_2O$ (**II**), have been synthesized (Scheme) and structurally characterized. Herein, we will present IR spectra, single-crystal X-ray diffraction, elemental analyses, and thermal analyses of the complexes **I** and **II**, anddescribe the coordination mode of o-$ClPhH_2IDC^-$ ligand (Fig. 1).

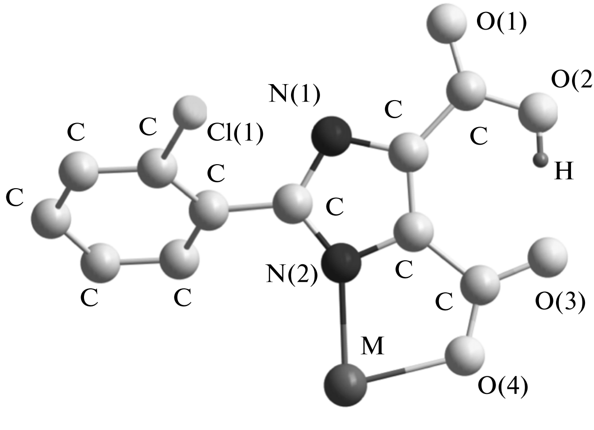

Fig. 1. Coordination mode of o-$ClPhH_2IDC^-$ anion.

---

[1] The article is published in the original.

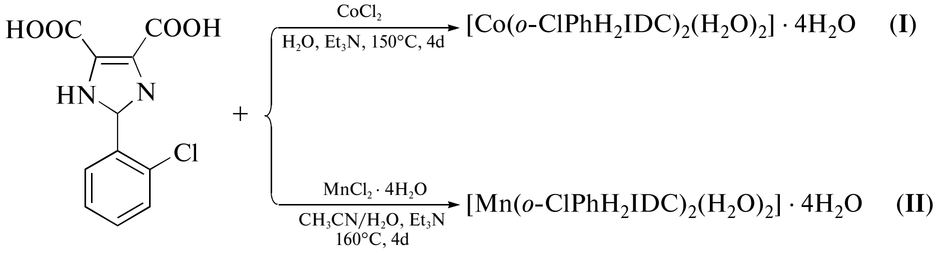

Scheme.

EXPERIMENTAL

Materials and methods. All chemicals were of reagent grade quality obtained from commercial sources and used without further purification. The organic ligand *o*-ClPhH$_3$IDC was prepared according to literature method [21]. The C, H, and N microanalyses were carried out on a FLASH EA 1112 analyzer. IR spectra were recorded on a BRUKER TENSOR 27 spectrophotometer as KBr pellets in the 400–4000 cm^{-1} region. TG measurements were performed by heating the crystalline sample from 30 to 850°C at a rate of 10°C min^{-1} in the air on a Netzsch STA 409PC differential thermal analyzer. X-ray powder diffraction (PXRD) measurements were recorded on a Panalytical X'pert PRO X-ray diffractometer.

Synthesis of I. A mixture of $CoCl_2 \cdot 6H_2O$ (23.8 mg, 0.1 mmol), *o*-ClPhH$_3$IDC (26.6 mg, 0.1 mmol), H_2O (7 mL), Et_3N (0.014 mL, 0.1 mmol) were sealed in a 25 mL Teflon-lined stainless steel autoclave, heated at 150°C for four days, and then cooled to room temperature. Amaranth orthorhombic crystals of **I** were isolated, washed with distilled water, and dried in air (69% yield based on Co).

IR (KBr; ν, cm^{-1}): 3418 s, 1722 m, 1548 s, 1471 s, 1385 m, 1290 m, 1128 w, 1060 m, 982 w, 740 m, 551 w.

For $C_{22}H_{24}N_4O_{14}ClCo$

anal. calcd., %:	C, 37.82;	H, 3.44;	N, 8.02.
Found, %:	C, 37.99;	H, 3.18;	N, 7.84.

Synthesis of II. A mixture of $MnCl_2 \cdot 4H_2O$ (20.2 mg, 0.1 mmol), *o*-ClPhH$_3$IDC (26.6 mg, 0.1 mmol), $CH_3CN–H_2O$ (3 : 4, 7 mL), Et_3N (0.014 mL, 0.1 mmol) were sealed in a 25 mL Teflon-lined stainless steel autoclave, heated at 150°C for four days, and then cooled to room temperature. Colorless orthorhombic crystals of **II** were isolated, washed with distilled water, and dried in air (58% yield based on Mn).

IR (KBr; ν, cm^{-1}): 3422 s, 1722 m, 1571 s, 1547 s, 1466 s, 1385 m, 1287 w, 1059 m, 980 w, 740 m.

For $C_{22}H_{24}N_4O_{14}ClMn$

anal. calcd., %:	C, 38.09;	H, 3.32;	N, 8.08.
Found, %:	C, 37.78;	H, 3.46;	N, 7.79.

X-ray crystallography. Measurements of compounds **I** and **II** were made on a Bruker smart APEXII CCD diffractometer with a graphite-monochromated MoK_α radiation (λ = 0.71073 Å). Single crystals of **I** and **II** were selected and mounted on a glass fiber. All data were collected at room temperature (296(2) K) using the ω–2θ scan technique and corrected for Lorenz-polarization effects. A correction for secondary extinction was applied. The two structures were solved by direct methods and expanded using the Fourier technique. The non-hydrogen atoms were refined with anisotropic thermal parameters. Hydrogen atoms were included but not refined. The final cycle of full-matrix least squares refinement was based on 6133 observed reflections and 440 variable parameters for **I**, 6181 observed reflections and 451 variable parameters for **II**. All calculations were performed using the SHELX-97 crystallographic software package [22]. Crystal data and experimental details for compounds **I** and **II** are contained in Table 1. The selected bond lengths and angles and hydrogen bonding parameters are listed in Table 2 and Table 3, respectively. Supplementary material has been deposited with the Cambridge Crystallographic Data Centre (nos. 1036900 and 1036899 for **I** and **II**, respectively; deposit@ccdc.cam.ac.uk or http://www.ccdc.cam.ac.uk).

RESULTS AND DISCUSSION

A single-crystal X-ray diffraction study shows that compound **I** is a mononuclear structure. An appropriate drawing of the molecular structure with atom labeling scheme is shown in Fig. 2a.

The asymmetric unit of **I** consists of central Co(II), two discrete *o*-ClPhH$_3$IDC anions, two coordinate waters and four free waters. The geometry around the Co(II) center is best portrayed as a distorted

Table 1. Crystallographic data and structural refinement information for compounds **I** and **II**

Parameter	Value	
	I	**II**
Fw	698.28	698.28
Crystal system	Triclinic	Triclinic
Crystal size, mm	0.22 × 0.21 × 0.18	0.24 × 0.18 × 0.16
Space group	$P\bar{1}$	$P\bar{1}$
a, Å	10.4974(5)	10.904(2)
b, Å	11.4488(6)	11.032(2)
c, Å	11.7474(6)	11.683(2)
α, deg	98.1520(10)	96.072(3)
β, deg	90.1610(10)	91.158(3)
γ, deg	97.4660(10)	94.055(3)
V, Å^3	1385.39(12)	1388.1(4)
ρ_{calcd}, mg m^{-3}	1.674	1.659
Z	2	2
μ, mm^{-1}	0.890	0.704
Reflections	8893/6133	8403/6181
Collected/unique (R_{int})	(0.0109)	(0.0391)
Data/restraints/parameters	6133/8/440	6181/21/451
GOOF on F^2	1.000	0.992
R	0.0265	0.0718
wR	0.0643	0.1984
$\Delta\rho_{max}$ and $\Delta\rho_{min}$, e Å^{-3}	0.585 and –0.582	1.266 and –2.168

$[CoO_4N_2]$ octahedral environment including two imidazole nitrogen (N(1) and N(3)) and two carboxylate oxygen atoms (O(4) and O(7)) from two individual *o*-$ClPhH_2IDC^-$ anions, and two oxygen atoms (O(5) and O(6)) from the coordinated water molecules (Fig. 2a). The Co–O distances span from 2.0478(12) to 2.1678(12) Å, while Co–N bond lengths are in the range of 2.1232(14)–2.1325(14) Å. In addition, within in the organic ligand, the dihedral angle between the imidazole ring and the phenyl plane is 51.5° indicating the serious twist. The two imidazole rings are parallel to each others, whose plane distance is 10.5823 Å. Two plane distances between the phenyl rings are 4.7511 and 6.9136 Å.

It should be point that both the *o*-$ClPhH_2IDC^-$ units and water molecules all participate in the formation of hydrogen bonds, especially the waters, which are an integral part of the crystal structure. Here is a view of the 3D structure of **I** (Fig. 2c). There are several types of hydrogen bonds in complex **I** (Table 3). The intramolecular H bonds consist of O(10)–H(10)···O(8) and O(2)–H(2)···O(3) between two carboxylate units of the same organic ligand. And the intermolecular H bond includes O(12)–H(20)···O(3), O(11)–H(23)···O(10), O(12)–H(21)···O(8), O(15)–H(52)···O(3), O(15)–H(53)···O(4) and O(14)–H(81)···O(1) between free waters and carboxyls of the ligands; O(5)–H(51)···O(9) and O(6)–H(6)···O(7) between the coordinate waters and carboxyls of ligands; N(4)–H(27)···O(11) and N(2)–H(28)···O(14) between N of the imidazole rings and the free waters; O(11)–H(22)···O(15) and O(14)–H(80)···O(15) between the free waters and O(6)–H(30)···O(14) and O(5)–H(5)···O(12) between the coordinate waters and the free waters. In order to express the connection method of various units more clearly, a 2D ladder-like plane of the supermolecular structure is showed in Fig. 2b. The neighbor $[Co(o\text{-}ClPhH_2IDC)_2(H_2O)_2]$ units are joined by the O–H···O H bonds (O(5)–H(51)···O(9) and O(6)–H(6)···O(7)) to form 1D jagged chains, and the intra-chain distances of adjacent Co(II) ions are 10.497, 5.358 and 9.164 Å. Furthermore, the 2D layer is constituted via the linkages of the hydrogen bonds N(4)–H(27)···O(1), O(11)–H(22)···O(15), O(14)–H(80)···O(15), O(15)–H(53)···O(4) and O(14)–H(81)···O(1) between the adjacent chains. Moreover, the layers are interlinked to produce a 3D

Table 2. Selected bond distances (Å) and angles (deg) for complexes **I** and **II**

Bond	*d*, Å	Bond	*d*, Å	Bond	*d*, Å
			I		
Co(1)–O(6)	2.0478(12)	Co(1)–O(5)	2.0479(12)	Co(1)–N(1)	2.1232(14)
Co(1)–N(3)	2.1325(14)	Co(1)–O(4)	2.1375(12)	Co(1)–O(7)	2.1678(12)
			II		
Mn(1)–O(17)	2.154(3)	Mn(1)–O(18)	2.180(3)	Mn(1)–O(8)	2.189(4)
Mn(1)–N(3)	2.226(4)	Mn(1)–O(4)	2.231(4)	Mn(1)–N(5)	2.277(4)
Angle	ω, deg	Angle	ω, deg	Angle	ω, deg
			I		
O(6)Co(1)O(5)	90.79(5)	O(6)Co(1)N(1)	163.06(5)	O(5)Co(1)N(1)	95.96(5)
O(6)Co(1)N(3)	90.12(5)	O(5)Co(1)N(3)	163.91(5)	N(1)Co(1)N(3)	87.67(5)
O(6)Co(1)O(4)	94.78(5)	O(5)Co(1)O(4)	85.84(5)	N(1)Co(1)O(4)	101.18(5)
N(3)Co(1)O(4)	78.07(5)	O(6)Co(1)O(7)	87.16(5)	O(5)Co(1)O(7)	88.87(5)
N(1)Co(1)O(7)	77.49(5)	N(3)Co(1)O(7)	107.22(5)	O(4)Co(1)O(7)	174.40(4)
			II		
O(17)Mn(1)O(18)	87.35(13)	O(17)Mn(1)O(8)	84.88(13)	O(18)Mn(1)O(8)	92.04(13)
O(17)Mn(1)N(3)	88.69(13)	O(18)Mn(1)N(3)	159.79(15)	O(8)Mn(1)N(3)	107.34(14)
O(17)Mn(1)O(4)	100.22(13)	O(18)Mn(1)O(4)	87.05(13)	O(8)Mn(1)O(4)	174.76(12)
N(3)Mn(1)O(4)	74.17(14)	O(17)Mn(1)N(5)	156.19(15)	O(18)Mn(1)N(5)	105.69(13)
O(8)Mn(1)N(5)	75.00(13)	N(3)Mn(1)N(5)	85.35(13)	O(4)Mn(1)N(5)	100.27(13)

solid-state framework by $\pi\cdots\pi$ stacking interactions of the phenyl rings (Fig. 2c). Notably, the hydrogen bonding interactions further stabilize the supramolecular network.

A single-crystal X-ray diffraction study shows that compound **II** is a mononuclear structure. A suitable drawing of the molecular structure with atom labeling scheme is shown in Fig. 3a.

The Mn^{2+} ion is six-coordinated, whose asymmetric unit contains central Mn^{2+} ion, two discrete *o*-$ClPhH_3IDC$-anions (N(3), N(5), O(4) and O(8)), two coordinate waters (O(17) and O(18)) and four free waters, adopting a distorted octahedral geometry $[MnO_4N_2]$. The Mn–O distances span from 2.154(3) to 2.231(4) Å, while Mn–N bond lengths are in the range of 2.226(4)–2.277(4) Å. All these are compared to those values in literatures [23, 24]. Moreover, within in the organic ligand, the dihedral angle between the imidazole ring and the phenyl plane is 50.0° indicating the serious twist. Two imidazole rings are parallel to each others, whose plane distance is 11.032 Å. There are two plane distances between the phenyl rings (4.5045 and 6.8527 Å).

Similarly, there are several kinds of hydrogen bonds in complex **II** (Table 3). The intermolecular H bonds consist of O(27)–H(11)···O(7), O(25)–H(9)···O(4); O(21)–H(10)···O(2) and O(23)–H(90)···O(5) between the free waters and the carboxyls of the imidazole rings; O(18)–H(18)···O(27); O(17)–H(15)···O(21) and O(18)–H(92)···O(23) between the coordinate waters and the free waters; N(4)–H(6)···O(23) and N(6)–H(13)···O(21) between N of the imidazole rings and the free waters; O(17)–H(15)···O(6) between the coordinate waters and carboxyls of ligands; O(21)–H(16)···O(27); O(23)–H(8)···O(25) and O(25)–H(17)···O(23) between the free waters and O(17)–H(20)···O(18) between the coordinate waters. The intramolecular H bonds includes O(5)–H(19)···O(7) between carboxyls of the same ligand. All these construct the supermolecular compound **II**, as it shows in Fig. 3c. The neighbor $[Mn(o\text{-}ClPhH_2IDC)_2(H_2O)_2]$ units are joined by the O–H···O H bonds (O(27)–H(11)···O(7), O(17)–H(20)···O(18), O(17)–H(15)···O(6), O(25)–H(9)···O(4), O(23)–H(8)···O(25), O(25)–H(17)···O(23), O(23)–H(90)···O(5) and O(18)–H(18)···O(27)) to form 1D straight chains, and the intra-chain distances of adjacent Mn^{2+} ions are 10.904, 5.252 and 9.365 Å. Furthermore, the 2D layer (Fig. 3b) is constituted via the linkages of the hydrogen bonds O(27)–H(7)···O(3), O(27)–H(11)···O(7) and O(21)–H(16)···O(27)) between the adjacent chains. Moreover, the layers are interlinked to produce a 3D framework $\pi\cdots\pi$ stacking interactions of the phenyl rings (Fig. 3c).

Table 3. Geometric parameters of hydrogen bonds for complexes **I** and **II**

D–H···A	Distance, Å			Angle DHA, deg
	D–H	H···A	D···A	
O(6)–H(6)···O(7)	0.82	2.08	2.879(1)	166
O(2)–H(2)···O(3)	0.82	2.53	1.708(3)	179
O(5)–H(5)···O(12)	0.82	2.72	1.899(2)	173
O(5)–H(51)···O(9)	0.81	2.01	2.783(1)	157
O(6)–H(30)···O(14)	0.83	1.95	2.773(2)	170
N(4)–H(27)···O(11)	0.81	1.91	2.721(1)	178
N(2)–H(28)···O(14)	0.82	2.11	2.913(1)	165
O(10)–H(10)···O(8)	0.82	2.50	1.685(2)	179
O(12)–H(21)···O(8)	0.83	2.09	2.893(1)	162
O(14)–H(81)···O(1)	0.86	1.91	2.755(2)	166
O(12)–H(20)···O(3)	0.84	2.12	2.910(2)	157
O(15)–H(52)···O(3)	0.81	2.10	2.905(1)	171
O(15)–H(53)···O(4)	0.86	2.08	2.940(1)	173
O(11)–H(22)···O(15)	0.81	2.05	2.864(2)	177
O(11)–H(23)···O(10)	0.81	2.31	3.118(3)	173
O(14)–H(80)···O(15)	0.81	2.31	3.034(1)	148
N(4)–H(6)···O(23)	1.06	1.75	2.785(2)	164
O(5)–H(19)···O(7)	0.77	1.68	2.495(1)	171
O(27)–H(7)···O(3)	0.82	2.15	3.001(2)	170
O(25)–H(9)···O(4)	0.81	2.00	2.844(1)	167
O(23)–H(8)···O(25)	0.82	1.90	2.728(2)	162
N(6)–H(13)···O(21)	0.77	2.14	2.883(1)	161
O(21)–H(10)···O(2)	0.86	2.07	2.905(1)	164
O(23)–H(90)···O(5)	0.81	2.21	3.010(1)	155
O(17)–H(15)···O(6)	0.85	2.26	2.898(1)	131
O(27)–H(11)···O(7)	0.85	1.99	2.781(2)	153
O(17)–H(15)···O(21)	0.85	2.29	2.850(1)	124
O(17)–H(20)···O(18)	0.83	2.20	3.010(2)	171
O(18)–H(18)···O(27)	0.86	1.98	2.778(2)	165
O(21)–H(16)···O(27)	0.82	2.20	2.997(1)	155
O(25)–H(17)···O(23)	0.81	1.93	2.728(2)	155
O(18)–H(92)···O(23)	0.81	2.04	2.880(3)	165

The strong and broad absorption bandsaround 3400–3500 cm^{-1} should be ascribed to the stretching vibrations of O–H and N–H, suggesting the presence of coordinated water molecules and imidazole ring, respectively. The asymmetric and symmetric stretching vibrations of carboxyl group in the complexes appeared at 1723 and 1548 cm^{-1} for **I**, 1722 and 1547 cm^{-1} for **II**, which can indicate the existence of free and coordinated carboxyl groups. The bands in the range of 600–800 cm^{-1} correspond to the benzene ring groups, respectively. In conclusion, IR spectra of **I** and **II** are consistent with the results of the X-ray diffraction analyses.

To confirm the phase purity of two supramolecules, the PXRD patterns were recorded. Most of the peak positions of simulated and measured patterns are in good agreement with each other, that is to say, the collected crystals were of great purity.

In order to estimate the thermal stabilities of the polymers, thermal gravimetric analyses of **I** and **II** were carried out in the air (Fig. 4). There are four-step of mass loss in **I**. The first weight loss from 30.2 to

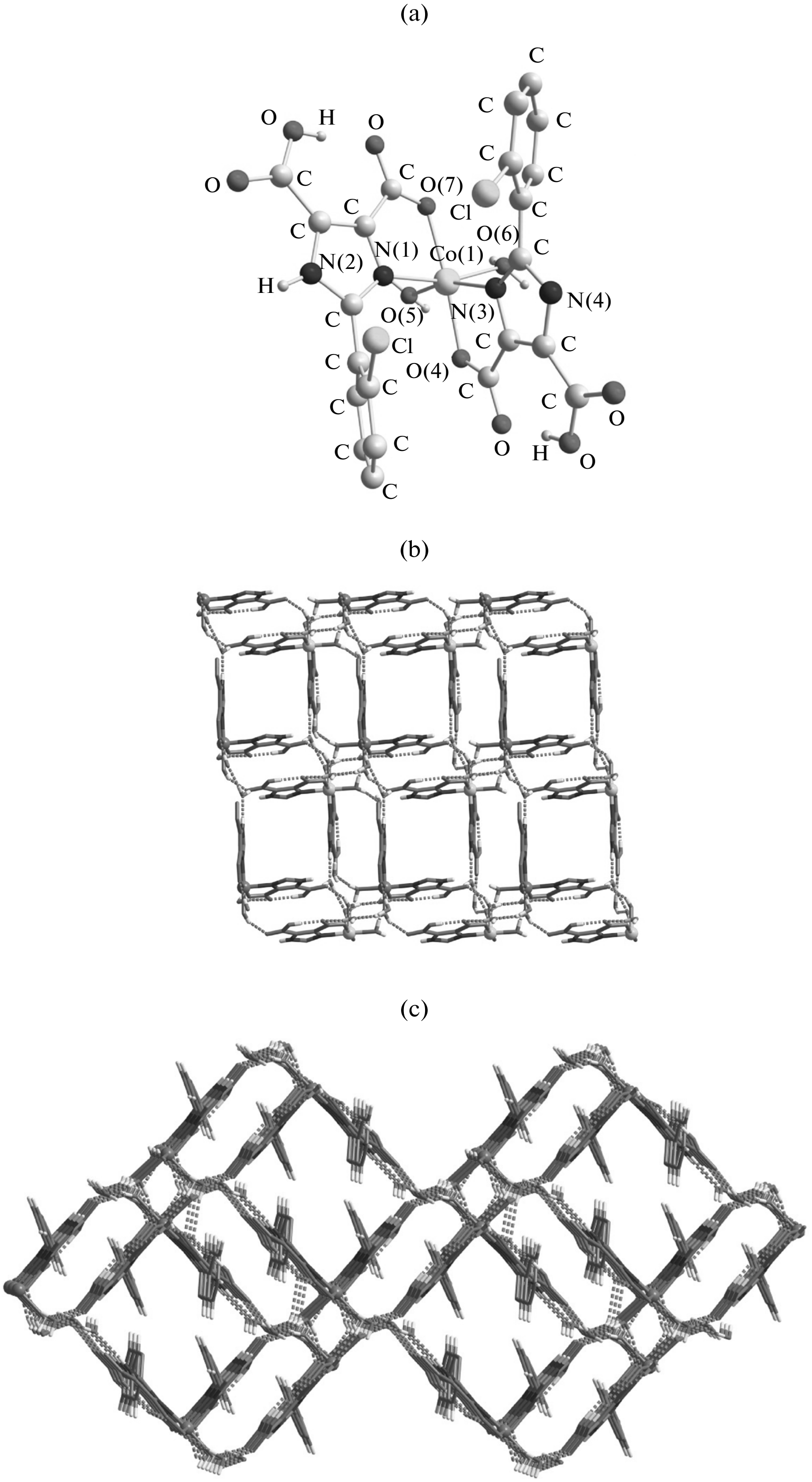

Fig. 2. Coordination environment of Co(II) atom in **I** (free water molecules omitted for clarity) (a); a planar structure of **I** (part H atoms and phenylgroups omitted for clarity) (b); a view of 3D supramolecular structure of **I** (c).

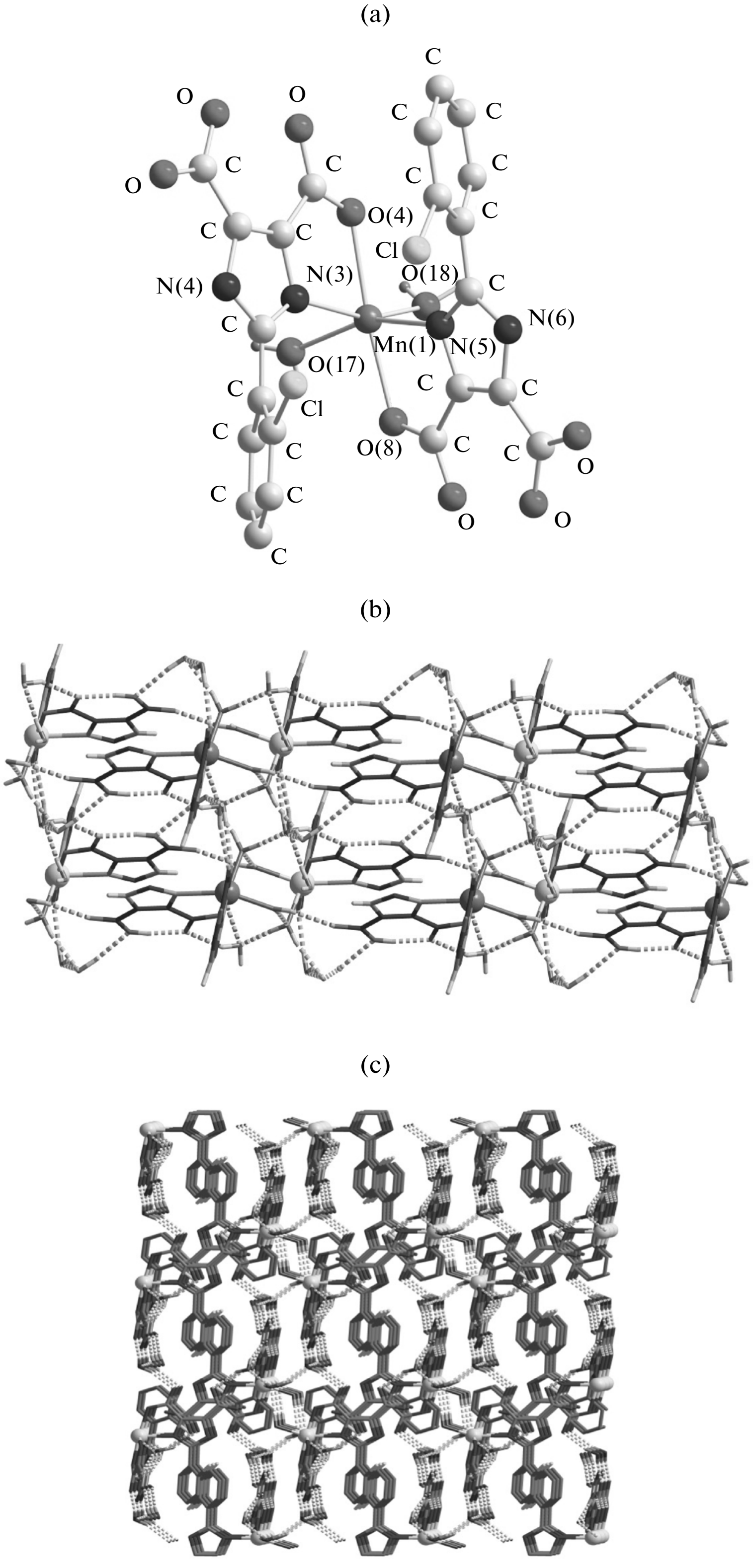

Fig. 3. Coordination environment of Mn(II) atom with atomic labels in **II** (free water molecules omitted for clarity) (a); a view of 2D supramolecular structure (part H atoms and phenylgroupsomitted for clarity) (b); 3D supramolecular structure of **II** showing the π–π stacking (c).

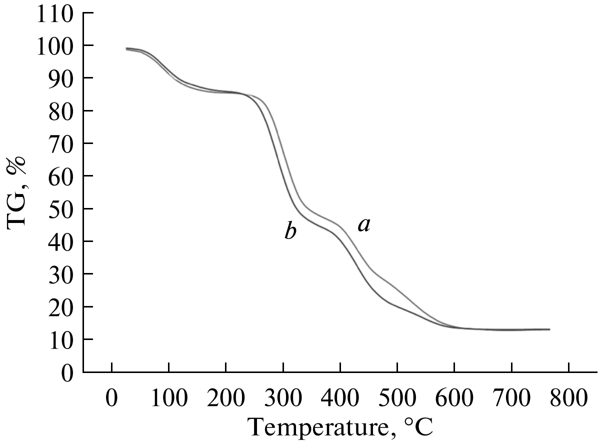

Fig. 4. TG analysis profiles of supramolecules **I** (*a*) and **II** (*b*).

187.5°C is corresponding to the weight loss of four free water molecules and two coordination water molecules (found 14.22%, calcd. 15.13%). Then, the organic ligand begins to collapse. With the release of the organic ligand, the second weight loss is 38.24% (calcd. 37.18%) from 187.5 to 335.0°C. It keeps losing weight from 335.2 to 632.5°C, which corresponds to the removal of the other organic ligand (found 36.22%, calcd. 37.18%). Finally, a plateau region is observed from 632.5 to 770.0°C. The remaining weight residue is CoO (found 11.32%, calcd. 10.49%).

Similarly, there is four-stage mass loss of supramolecule **II**. The first weight loss from 29.98 to 197.5°C corresponds to the weight loss of three free water molecules and two coordination water molecules (found 13.78%, calcd. 12.89%). Then, the organic ligand begins to collapse, at the same time, the residual coordination water molecule sloughs from 202.5 to 372.5°C (found 41.68%, calcd. 39.15%). Next, with the release of the second organic ligand, it keeps losing weight from 372.5 to 695.0°C (found 32.65%, calcd. 36.62%). Finally, a plateau region is revealed from 695.0 to 770.0°C. The remaining weight of 10.89% corresponds to the percentage (calcd. 10.00%) of the Mn and O components, indicating that the final residue is MnO.

In this work, two transition metal supramolecules **I** and **II** have been successfully prepared under hydro(solvo)thermal conditions. Their crystal structures have been characterized by single-crystal X-ray diffraction. To characterize the complexes more fully, their thermal behaviors were studied by thermal gravimetric analyses. The 3D supramolecular architectures reveal the strong coordination ability of the *o*-$ClPhH_3IDC$ ligand. However, some oxygen and nitrogen atoms in *o*-$ClPhH_3IDC$ are not involved in the coordination directly; the hydrogen-bond interactions of the *o*-$ClPhH_3IDC$ ligand are involved in the solid state packing.

ACKNOWLEDGMENTS

We gratefully acknowledge the financial support by the National Natural Science Foundation of China (nos. 21341002 and J1210060) and the Natural Science Foundation of Henan Education Department (13A150655).

REFERENCES

1. Sculley, J., Yuan, D., and Zhou, H.C., *Energy Environ. Sci.*, 2011, vol. 4, p. 2721.
2. Liu, J., Thallapally, P.K., McGrail, B.P., et al., *Chem. Soc. Rev.*, 2012, vol. 41, p. 2308.
3. Pluth, M.D., Bergman, R.G., and Raymond, K.N., *Chem. Res.*, 2009, vol. 42, p. 1650.
4. Liu, T.F., Lu, J., Tian, C., et al., *Inorg. Chem.*, 2011, vol. 50, p. 2264.
5. Bai, Y.L., Tao, J., Huang, R.B., and Zheng, L.S., *Angew. Chem. Int. Ed.*, 2008, vol. 47, p. 5344.
6. Ma, S., Yuan, D., Wang, X.S., and Zhou, H.C., *Inorg. Chem.*, 2009, vol. 48, p. 2072.
7. Wang, Z.X., Wu, Q.F., Liu, H.J., et al., *CrystEngComm*, 2010, vol. 12, p. 1139.
8. Liu, G.Z., Wang, J.G., and Wang, L.Y., *CrystEngComm*, 2012, vol. 14, p. 951.
9. Zhang, X.M., Hao, Z.M., Zhang, W.X., and Chen, X.M., *Angew. Chem. Int. Ed.*, 2007, vol. 46, p. 3456.
10. Song, Y.J., Kwak, H., Lee, Y. M., et al., *Polyhedron*, 2009, vol. 28, p. 1241.
11. Ludovic, C., Bruno, T., and Georg, S.F., *J. Organomet. Chem.*, 2006, vol. 691, p. 4257.
12. Rishi, G.V., Agenor, L., Jorge, M.R.R., et al., *Bioorg. Med. Chem. Lett.*, 2009, vol. 19, p. 132.
13. Gu, Z.G., Liu, Y.T., Hong, X.J., et al., *Cryst. Growth Des.*, 2012, vol. 12, p. 2178.
14. Cai, S.L., Zheng, S.R., Wen, Z.Z., et al., *Cryst. Growth Des.*, 2012, vol. 12, p. 3575.
15. Sun, Y.G., Yu, W., Wang, L., et al., *Russ. J. Coord. Chem.*, 2010, vol. 36, p. 43.
16. Zhao, B., Zhao, X.Q., Shi, W., and Cheng, P.J., *Mol. Struct.*, 2007, vol. 830, p. 143.
17. Wang, W.W., Niu, X.L., Gao, Y.C., et al., *Cryst. Growth Des.*, 2010, vol. 10, p. 4050.
18. Cao, X., Zhang, J.J., Wang, C.J., et al., *CrystEngComm*, 2012, vol. 14, p. 4357.
19. Zhang, Y., Luo, X.B., Yang, Z.L., and Li, G., *CrystEngComm*, 2012, vol. 14, p. 7382.
20. Li, Z.F., Luo, X.B., Gao, Y.C., et al., *Inorg. Chim. Acta*, 2012, vol. 384, p. 352.
21. Lebedev, A.V., Lebedeva, A.B., Sheludyakov, V.D., et al., *Russ. J. Gen. Chem.*, 2007, vol. 77, p. 855.
22. Sheldrick, G.M., SHELX-97, Göttingen (Germany): Univ. of Göttingen, 1997.
23. Pachfule, P., Das, R., Poddar, P., and Banerjee, R., *Inorg. Chem.*, 2011, vol. 50, p. 3855.
24. Yi, F.Y. and Sun, Z.M., *Cryst. Growth Des.*, 2012, vol. 12, p. 5693.